

Comparative Evaluation of Bone and Some Materials Used as Bone Tissue Substitutes in Radiotherapy and Radiological Applications

Kelechi K. Ochommadu, *Nwamaka I. Akpu, Okhuomaruyi D. Osahon

Received: 26 November 2024/Accepted: 02 March 2025/Published: 14 March 2023

<https://dx.doi.org/10.4314/cps.v12i3.15>

Abstract: In this work, a study of radiation scattering properties of some real bone tissues and bone tissue-equivalent materials was carried out. The selected real bone tissues which are six in number include cortical bone, humerus, mandible, cartilage, yellow marrow and spongiosa. The tissue-equivalent materials include red marrow/G1, red marrow/L3, red marrow/SR4, aluminium, Cameron wax, facey liquid, magnesium, plaster of Paris, poll resin, poly (vinyl chloride), pyrex, Shonka plastic (B100) and Spiers liquid. Monte-Carlo software package (EGSnrc) was used to determine and study the scattering properties of the selected real bone tissue and its substitutes with the view of establishing an equivalence between them. The simulation of the transport of X-ray photons considered photoelectric absorption, coherent scattering and Compton scattering. The incident photon energy used in the simulation of angular distributions of photons scattered by these bone tissues is 17.44 keV. The computational result shows that the scattering properties of some of the bone tissue equivalent materials are similar to some of the real bone tissues. It revealed that the peak positions for real bone tissues: cortical bone, cartilage, yellow marrow and spongiosa gotten from the angular dispersive scattering studies were found to occur at 0.19286 \AA^{-1} , 0.17331 \AA^{-1} , 0.1341 \AA^{-1} and 0.3667 \AA^{-1} respectively. Those obtained from the bone tissue-equivalent materials: magnesium, red marrow/G1 and Cameron wax are 0.19286 \AA^{-1} , 0.23186 \AA^{-1} and 0.17331 \AA^{-1} respectively. As a result of closeness in the scattering properties, it was concluded that magnesium and poll resin bone tissue substitutes can simulate the cortical bone

tissue. Red marrow/G1, red marrow/L3 and Cameron wax bone tissue substitutes can be used to simulate the cartilage bone tissue. Red marrow/S4 and Cameron wax bone tissue substitutes are good substitutes for yellow marrow bone tissue while pyrex is not a good substitute for any of the bones. Based on the wide disparity in scattering properties studies obtained in this work, it was not possible to identify a good substitute for the humerus, mandible and spongiosa real bone tissues from among the selected tissue equivalent materials.

Keywords: X-ray Coherent Scattering; Bone tissue; Photon Transport; EGSnrc Monte Carlo code.

Kelechi K. Ochommadu

Department of Physics, Michael Okpara University of Agriculture, Umudike, P.M. B. 7267. Umuahia, Abia State.

ochommadu.kelechi@mouau.edu.ng

Orcid id: 0009-0004-4570-9133

Nwamaka I. Akpu*

Department of Physics, Michael Okpara University of Agriculture, Umudike, P.M. B. 7267. Umuahia, Abia State.

Akpu.nwamaka@mouau.edu.ng

Orcid id: 0000-0001-8062-9279

Okhuomaruyi D. Osahon

Department of Physics, University of Benin, Benin City, Nigeria

Email: Okhuomaruyi.osahon@uniben.edu

1.0 Introduction

In radiotherapy and radiological applications, accurate tissue simulation is crucial for optimizing treatment planning, dose calculations, and quality assurance. Bone tissue

plays a significant role in radiation transport, as its higher density and atomic composition influence photon absorption, scattering, and secondary radiation effects. As direct experimentation on human tissues is often impractical, tissue-equivalent materials are commonly used to replicate the physical and radiological properties of real bone tissues (Ferreira *et al.*, 2010). These substitutes aid in dosimetry, imaging system calibration, and radiotherapy planning, ensuring accurate patient treatment while minimizing unnecessary radiation exposure (Jones *et al.*, 2003; Hintenlang *et al.*, 2003; Bolch *et al.*, 2003).

An ideal bone tissue substitute should closely match real bone in elemental composition, density, mass attenuation coefficient (TMAC), and scattering characteristics. While some materials have been developed for soft tissues, finding suitable substitutes for bone remains a challenge, particularly in applications involving high-energy X-rays used in radiotherapy and diagnostic imaging. Scattering properties, which influence radiation penetration and dose distribution, are critical factors in determining the suitability of substitute materials. For two materials to be considered true equivalents, they must exhibit similar photon scattering profiles, ensuring comparable interactions with ionizing radiation (Poletti *et al.*, 2004; Goncalves *et al.*, 2004; Mazzaro *et al.*, 2004; Bozkurt *et al.*, 2023).

To study the scattering properties of different bone-equivalent materials, Small Angle X-ray Scattering (SAXS) has been widely employed. SAXS is a powerful X-ray diffraction technique that analyzes the structural characteristics of biological tissues, polymers, and other complex materials (Sibillano *et al.*, 2014). Unlike conventional X-ray crystallography, which requires highly ordered structures, SAXS provides molecular-level insights into disordered and amorphous biological tissues, making it suitable for studying bone and its substitutes. The

technique involves directing a collimated beam of X-rays at a sample and measuring the coherent (elastic) scattering at small angles, producing a unique scattering signature characteristic of the material. The momentum transfer (q) that defines this scattering behaviour is given by:

$$q = \frac{\sin(\frac{\theta}{2})}{\lambda} yea, I \quad (1)$$

where λ is the wavelength of the incident photon, and θ is the scattering angle. The interference of scattered X-ray photons generates a diffraction pattern that provides information about the molecular composition and density of the target tissue.

Previous studies have used SAXS to evaluate tissue-equivalent materials in mammography and conventional radiology, showing variations in scattering profiles between biological tissues and their synthetic substitutes (Poletti *et al.*, 2004; Goncalves *et al.*, 2004; Mazzaro *et al.*, 2004). Harding *et al.* (1987) reported that fat and bone exhibit significantly different scattering signatures compared to soft tissues such as muscle and liver, which has implications for radiation dose calculations. Similarly, Evans *et al.* (1991) and Bradley *et al.* (1991) investigated coherent scattering in breast tissue and water-based substitutes, while Kidane *et al.* (1999) demonstrated the sensitivity of X-ray scattering to molecular-level variations in biological materials.

Despite these advancements, identifying bone-equivalent materials that accurately replicate real bone scattering properties for radiotherapy applications remains a challenge. This study aims to address this gap by conducting a comparative evaluation of bone and selected substitute materials, analyzing their scattering behavior using Monte Carlo simulations (EGSnrc). Monte Carlo methods provide an efficient computational approach for modeling low-angle X-ray scattering, offering a cost-effective alternative to experimental techniques. By examining the angular distribution of scattered photons, this study seeks to determine the suitability of different



bone tissue substitutes for use in radiotherapy and radiological applications.

2.0 Materials and Methods

In this study, Monte Carlo simulations were employed to investigate the scattering properties of selected real bone tissues and various tissue-equivalent materials. The Monte Carlo software package EGSnrc was used for the simulations, and a customized user code named KINGS was developed and executed for the computations. The selected real bone tissues and their substitute materials are listed in Table 1, while their elemental compositions and mass densities are presented in Tables 2 and 3, respectively.

Table 1. Real Bone Tissues and Substitute Materials considered in this work

Real Bone	Bone	Tissue
	Substitutes	
Cortical bone, Humerus, Mandible, Cartilage, Yellow marrow and Spongiosa	RM/G1, RM/SR4, Cameron wax, liquid, Plaster of paris, resin, poly(vinyl chloride), Pyrex, Shonka plastic (B100) and Spiers liquid.	RM/L3, Aluminium, Facey Magnesium, Poll poly(vinyl chloride), Pyrex,

Table 2: Elemental Compositions and Mass Density (ρ) of the Real Bone Tissues (Values are given as percentage by mass)

Tissue	H	C	N	O	Others	Density (kg/m ³)
Cortical bone	3.4	15.5	4.2	43.5	0.1 Na, 0.2 Mg, 10.3 P, 0.3 S, 22.5 Ca	1920
Humerus	6.0	31.4	3.1	36.9	0.1 Na, 0.1 Mg, 7.0 P, 0.2 S, 15.2 Ca	1460
Mandible	4.6	19.9	4.1	43.5	0.1 Na, 0.2 Mg, 8.6 P, 0.3 S, 18.7 Ca	1680
Cartilage	9.6	9.9	2.2	74.4	0.5 Na, 2.2 P, 0.9 S, 0.3 Cl	1100
Yellow Marrow	11.5	64.4	0.7	23.1	0.1 Na, 0.1 S, 0.1 Cl	980
Spongiosa	8.5	40.4	2.8	36.7	0.1 Na, 0.1 Mg, 3.4 P, 0.2 S, 0.2 Cl, 0.1 K, 7.4 Ca, 0.1 Fe	1180

The Monte Carlo simulations accounted for photoelectric absorption, coherent (Rayleigh) scattering, and Compton scattering to provide a comprehensive analysis of the scattering interactions. The transport of photons and electrons was tracked until their energies reached predefined energy cut-off values. These cut-offs were set as follows: AE = 0.512 MeV, AP = 0.001 MeV, ECUT = 0.621 MeV, and PCUT = 0.001 MeV, based on the definitions provided by Nelson *et al.* (1980). The fractional atomic weights (cross-sections) of each bone tissue substitute were determined

using PEGS4 codes, as described by Nelson *et al.* (1980).

To ensure accurate tissue modelling, the elemental compositions were referenced from ICRU Report 44 and ICRU Report 46, which provide standardized descriptions of human tissues. The incident photon energy used for the simulations was 17.44 keV, representing an X-ray photon from a molybdenum (Mo) tube operating at 30 kVp, which closely approximates a monochromatic X-ray beam suitable for bone tissue analysis. The thickness of each scatterer was set at 2.54 μm to optimize scattering interactions.



The Monte Carlo simulations followed the random paths of photons through the tissue substitutes until they were either absorbed or scattered. The study classified transmitted photons into primary, Compton scatter, Rayleigh scatter, or those absorbed via the photoelectric effect. These classifications were analyzed using a 2 keV energy bin interval. Additionally, the energy and angular distributions of the scattered photons were

computed separately for Compton and Rayleigh scattering categories. Angular distributions were analyzed in 2° angular bins for both real bone and substitute materials. To minimize statistical uncertainty and enhance the reliability of the results, several million photon histories were simulated in multiple batches, ensuring a well-distributed data set for each material thickness.

Table 3: Elemental Compositions and Mass Density (ρ) of the Bone Tissue Substitutes
(Values are given as percentage by mass)

Substitute Material	H	C	N	O	Others	Density (kg/m ³)
RM/G1	10.2	9.4	2.4	77.4	0.1 Na, 0.1 S, 0.2 Cl, 0.2 K, trace 0.03 P	1070
RM/L3	10.2	12.8	2.2	74.1	0.1 Na, 0.2 S, 0.2 Cl, 0.2 K, trace 0.03 P	1040
RM/SR4	10.1	73.6	2.2	13.7	0.1 S, 0.1 Cl, 0.2 K, traces 0.03 P, 0.01 Na, 0.003 Mg	1030
Aluminium	-	-	-	-	100% Al	2700
Cameron wax	8.62	54.42	-	20.14	-	1280
Facey Liquid	5.04	-	-	39.96	19.86 Ca	1420
Magnesium	-	-	-	-	100% Mg	1740
Plaster of Paris	15.0	-	-	55.8	18.6 S, 23.3 Ca	2320
Poll resin	4.09	16.3	80.51	47.09	13.92 P, 18.01 Ca	1880
P.V.C	4.8	38.5	-	-	56.7 Cl	1350
Pyrex	-	-	-	53.96	4.01 B, 2.82 Na, 10.03 Ca, 39.98 Br	2200
Shonka plastic (B100)	6.51	54.24	2.26	2.59	16.74 F, 17.66 Ca	1450
Spiers liquid	5.60	44.41	-	-	10.03 Ca, 39.98 Br	1530

3.0 Results and Discussions

3.1 Comparison of the angular dispersive x-ray scattering patterns for the real bone tissues and the bone tissue substitutes

The intensity versus momentum transfer (Å^{-1}) plots (Fig. 1a–1f) illustrate the scattering behavior of different materials under study. These figures provide insights into the structural properties, particle distribution, and interaction effects within the samples. The results are presented as a function of

momentum transfer argument q . All of the patterns were normalized to 1. The primary observations include variations in peak positions, intensities, and broadening effects, which can be linked to morphological differences and sample compositions.

Fig. 1a presents scattering data for CTB, MG, PR, SPL, and CAM samples. The peak positions for these real bone tissue (Cortical bone) and that of the bone tissue equivalent materials (Magnesium, Poll resin) were found



to occur at same momentum transfer (x) value of 0.19286 \AA^{-1} . Both bone tissue equivalent materials are very similar in overall features (shape and peak positions) as shown in the figures with the Cortical bone tissue. While the ones of Spiers Liquid and Cameron wax were found to occur at 0.27067 \AA^{-1} and 0.17331 \AA^{-1} respectively. The observed intensity profiles exhibit similar peak trends with noticeable variations in scattering intensity, suggesting differences in particle size and density. The peak at lower momentum transfer values indicates larger particle sizes, while variations in peak height suggest different levels of structural ordering or aggregation. These results were similar to the X-ray diffraction patterns measured by Poletti *et al.*, 2004 for cortical bone tissue in terms of its peak position (see Table 4).

Fig. 1b displays scattering profiles for HUM, MG, PR, SPL, and CAM. The trend is comparable to Fig. 1a, but with subtle differences in intensity distribution. The presence of multiple overlapping peaks suggests a range of particle sizes and a polydisperse nature of the samples. The CAM sample appears to have the highest peak intensity, implying strong scattering due to either higher electron density contrast or better-defined nanostructures.

Fig. 1c includes MAND, PVR, PR, SPL, and B100. The peak positions for the real bone tissue (Mandible) and that of the Pyrex and Shonka plastic (bone tissue equivalent materials) were found to occur at the same momentum transfer (x) value of 0.23186 \AA^{-1} . Pyrex and Shonka plastic show the same scattering profile different only in magnitude, meaning similar structural properties. While the ones of Spiers Liquid and Poll resin were found to occur at 0.27067 \AA^{-1} and 0.19286 \AA^{-1} respectively. This shows that Spiers Liquid and Poll resin are bad simulators of Mandible tissue. The overall shape of the curves is consistent with previous figures; however, there is a shift in peak positions, indicating

structural modifications or compositional variations. The B100 sample exhibits the most distinct scattering pattern, potentially due to a different crystallinity or particle dispersion in the medium. The result for mandible was seen to agree with that of Chaparian *et al.*, (2012) (see Table 4). Small differences can be explained based on momentum transfer resolution of the system.

Fig. 1d showcases scattering data for CART, RMG, RML3, CAM, B100, and PVC. The peak positions for the Cartilage (real bone tissue) and those of the RM/G1, RM/L3, and Cameron wax (bone tissue equivalent materials) were found to occur at the same momentum transfer (x) value of 0.17331 \AA^{-1} . The X-ray diffraction patterns obtained in this study were in good agreement with previous measurements in terms of the peak position of bone tissue. The peak positions of P.V.C and Shonka plastic (B100) occur at 0.21236 \AA^{-1} and 0.23186 \AA^{-1} respectively. The result for Cartilage agrees with that of Chaparian *et al.*, 2012. (see Table 4). The presence of multiple peaks suggests a more complex microstructure within these materials. The CART and RMG samples display relatively smooth intensity decay, indicative of a well-dispersed and homogenous structure, whereas the PVC sample exhibits sharper peaks, hinting at ordered domains or larger structural units.

Fig. 1e represents SPONG, MG, AL, and POP. The peak positions for the real bone tissue-Spongisa was found to occur at momentum transfer (x) value of 0.3667 \AA^{-1} . While the ones of Magnesium were found to occur at 0.19286 \AA^{-1} , and that of aluminium and Plaster of paris were found to occur at the same momentum transfer of 0.21238 \AA^{-1} respectively. These results show that Magnesium, Aluminium and Plaster of Paris are bad simulators of Spongisa. The results for Aluminium did not agree with those of Barroso *et al.*, 2000 and Swanson 1953. The SPONG sample shows the highest intensity among the group, suggesting a more pronounced



scattering effect, potentially due to porous structures or high electron density differences. The MG and AL samples exhibit more gradual

intensity decreases, possibly indicating smoother and more dispersed particle distributions.

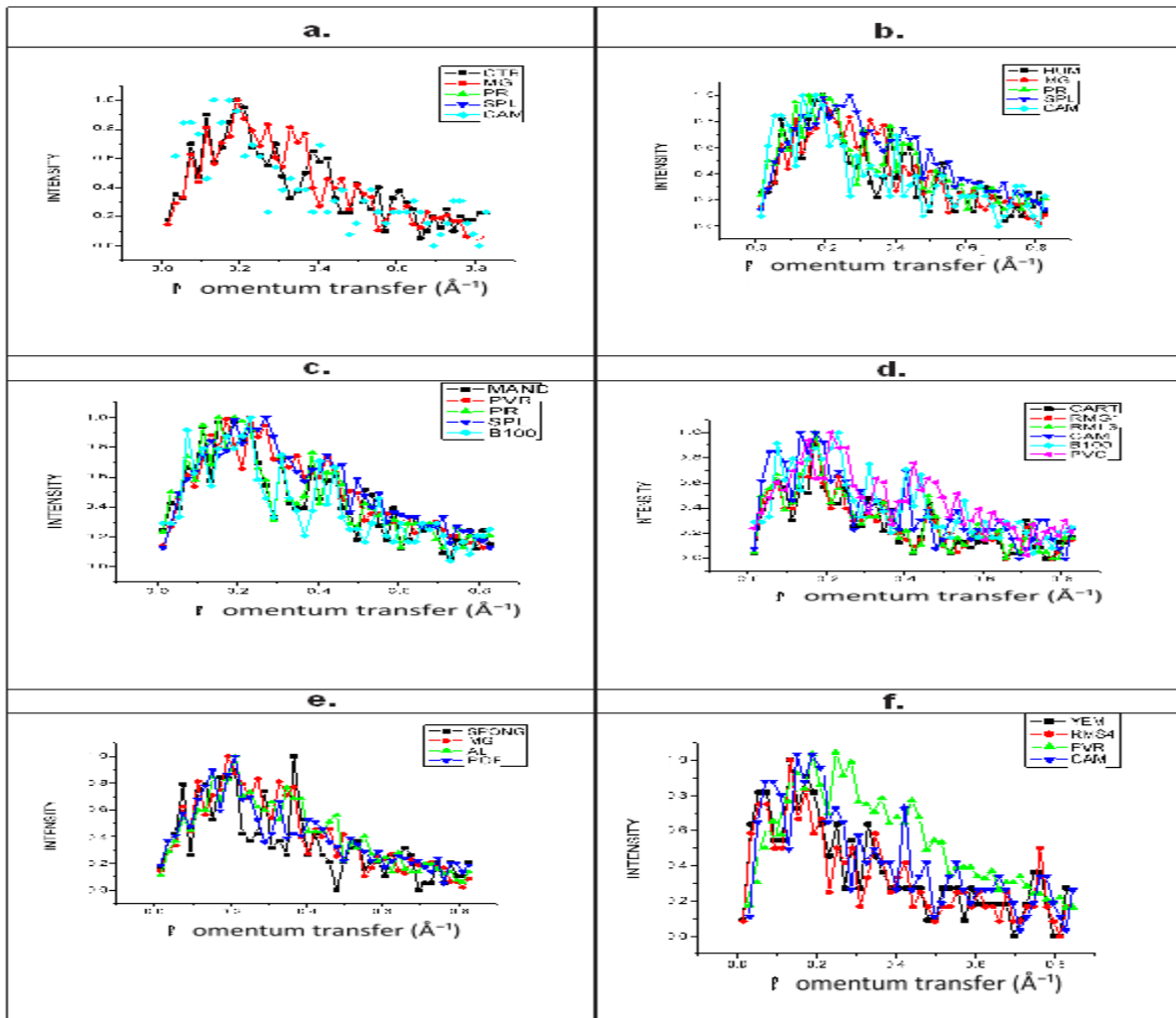


Fig. 1: The comparison of the scattering signatures for the real bone tissues (a) Cortical bone (b) Humerus (c) Mandible (d) Cartilage (e) Yellow Marrow and bone tissue substitute materials

¹CTB- Cortical bone

¹HUM- Humerus

¹MAND-Mandible

¹CART- Cartilage

¹YEM- Yellow marrow

¹SPONG-Spongisa chloride)

*MG- Magnesium

*PR- Poll Resin

*SPL- Spiers Liquid

*CAM- Cameron wax

*PVR- Pyrex

*B100- Shonka Plastic

*RMG1- Red marrow /G1

*RML3- Red marrow /L3

*RMS4- Red marrow/S4

*AL- Aluminium

*PVC- Poly (vinyl

¹ -Real bone tissues

* - Bone tissue equivalent materials



Fig. 1f displays data for YEM, RMS4, PVR, and CAM. The peak positions for the real bone tissue (Yellow marrow) and that of the RMS4 and Cameron wax (bone tissue equivalent materials) were found to occur at same momentum transfer (q) value of 0.1341 \AA^{-1} . While the one of Pyrex was found to occur at 0.17331 \AA^{-1} . These results show that Yellow marrow can very well be simulated by RM/S4 and Cameron wax while Pyrex is a bad simulator. The variations in peak heights and positions suggest differences in particle size distribution. The CAM sample, as seen in previous figures, maintains a high-intensity profile, reinforcing its distinct scattering characteristics. The RMS4 sample shows a broader peak, which may be attributed to an amorphous or less ordered structure. Across all six subfigures, common trends include:

- The presence of distinct peaks at lower momentum transfer values, indicating larger particle sizes.
- Variation in peak intensities, suggesting differences in electron density contrast and material composition.
- Broader peaks in some samples, hinting at amorphous structures or polydisperse distributions.

These findings suggest that the materials analyzed exhibit a range of morphological features, with some showing crystalline-like structures while others appear more amorphous. The CAM sample, appearing in multiple sub-figures, consistently shows high scattering intensity, which may be due to its composition or structural arrangement.

Table 4: The peak positions of the simulated X-ray scattering profile for the real bone tissues and the bone tissue substitutes obtained in this study compared with those reported earlier in the literature.

Real Bone	Peak Positions q (\AA^{-1})			Bone Substitutes	Peak Positions q (\AA^{-1})		
	This work	Poletti <i>et al.</i> 2004	Chaparian <i>et al.</i> 2012		This work	Barroso <i>et al.</i> 2000	Swanson 1953
Cortical bone^a	0.19286	0.19286	NA	Magnesium ^b	0.19286	NA	NA
Humerus^a	0.19286	NA	NA	Poll Resin ^b	0.19286	NA	NA
Mandible^a	0.23186	NA	0.23±0.115	Spiers Liquid ^b	0.27067	NA	NA
				Cameron Wax ^b		NA	NA
				Pyrex ^b	0.23186	NA	NA
				Shonka Plastic ^b	0.23186	NA	NA
Cartilage^a	0.17331	NA	0.16±0.08	Poll Resin ^b	0.19286	NA	NA
				Spiers Liquid ^b	0.19286	NA	NA
				RM/G1 ^b	0.17331	NA	NA
				RM/L3 ^b	0.17331	NA	NA



				Shonka Plastic ^b	0.23186	NA	NA
Yellow Marrow^a	0.1341	NA	NA	RM/S4 ^b	0.1341	NA	NA
				Cameron Wax ^b	0.1341	NA	NA
				Pyrex ^b	0.17331	NA	NA
				Spiers Liquid ^b	0.27067	NA	NA
Spongiosa^a	0.3667	NA	NA	Magnesium ^b	0.19286		
				Aluminium ^b	0.21238	0.3434	0.3494
				Plaster of Paris ^b	0.21238	NA	NA
				Cameron wax ^b	0.17331	NA	NA

a = Value corresponding to real bone, b = Value corresponding to bone tissue substitutes
NA Not available

3.2 Comparison between the number of photons transmitted as primary, Rayleigh, and total scatter

The comparison of photons transmitted as primary, Rayleigh, and total scatter for real bone tissue and bone tissue-equivalent materials is presented in Figs. 2–4.

Fig. 2 shows the percentage differences in primary scatter for various materials compared to different bone tissues. For cortical bone, Magnesium, Poll resin, Spiers Liquid, and Cameron wax show differences of 0.00021%, 0.007274%, 0.104393%, and 0.015566%, respectively. When compared to the humerus, the values are 0.00251%, 0.009578%, 0.106694%, and 0.0106694%. For the mandible, Pyrex, Shonka plastic, Poll resin, and Spiers Liquid exhibit differences of 0.1400478%, 0.0063534%, 0.003765%, and 0.100886%. Cartilage comparisons with RM/G1, RML3, Cameron wax, PVC, and Shonka plastic yield 0.00067%, 0.00078%, 0.001393%, 0.157643%, and 0.0112674%. Yellow marrow comparisons with RM/S4, Cameron wax, and Pyrex give 0.000036%, 0.000524%, and 0.1595568%. Spongiosa comparisons with Magnesium, Aluminium, and Plaster of Paris yield 0.01046%, 0.02685%, and 0.02949%.

Fig. 3 illustrates the percentage differences in Rayleigh scatter. For cortical bone, Magnesium, Poll resin, Spiers Liquid, and Cameron wax have differences of 19.5767%, 5.952331%, 93.78307%, and 73.28042%, respectively. Comparisons with the humerus show differences of 75.1938%, 55.23256%, 95.81%, and 60.85271%. Cartilage comparisons with RM/G1, RM/L3, Cameron wax, PVC, and Shonka plastic result in 9.053498%, 13.058025%, 16.87243%, 734.97942%, and 97.119342%. Yellow marrow comparisons with RM/S4, Cameron wax, and Pyrex yield 1.35135%, 36.48649%, and 1270.9459%. Spongiosa comparisons with Magnesium, Aluminium, and Plaster of Paris result in 133.22%, 95.84%, and 110.40%.

Fig. 4 presents total scatter percentage differences. For cortical bone, Magnesium, Poll resin, Spiers Liquid, and Cameron wax exhibit 8.86427%, 4.339796%, 59.926%, and 55.86334%. Comparisons with the humerus show differences of 55.5409%, 49.07652%, 128.496%, and 36.93931%. Mandible comparisons with Pyrex, Shonka plastic, Poll resin, and Spiers Liquid yield 145.8031%, 24.0415%, 17.09845%, and 79.4819%. Cartilage comparisons with RM/G1, RM/L3, Cameron wax, PVC, and Shonka plastic give



1.931330%, 6.866953%, 2.575107%, 409.01288%, and 57.296135%. Yellow marrow comparisons with RM/S4, Cameron wax, and Pyrex show 1.40845%, 34.64789%, and 568.16901%. Finally, Spongiosa

comparisons with Magnesium, Aluminium, and Plaster of Paris result in 113.079%, 75.15%, and 95.15%.

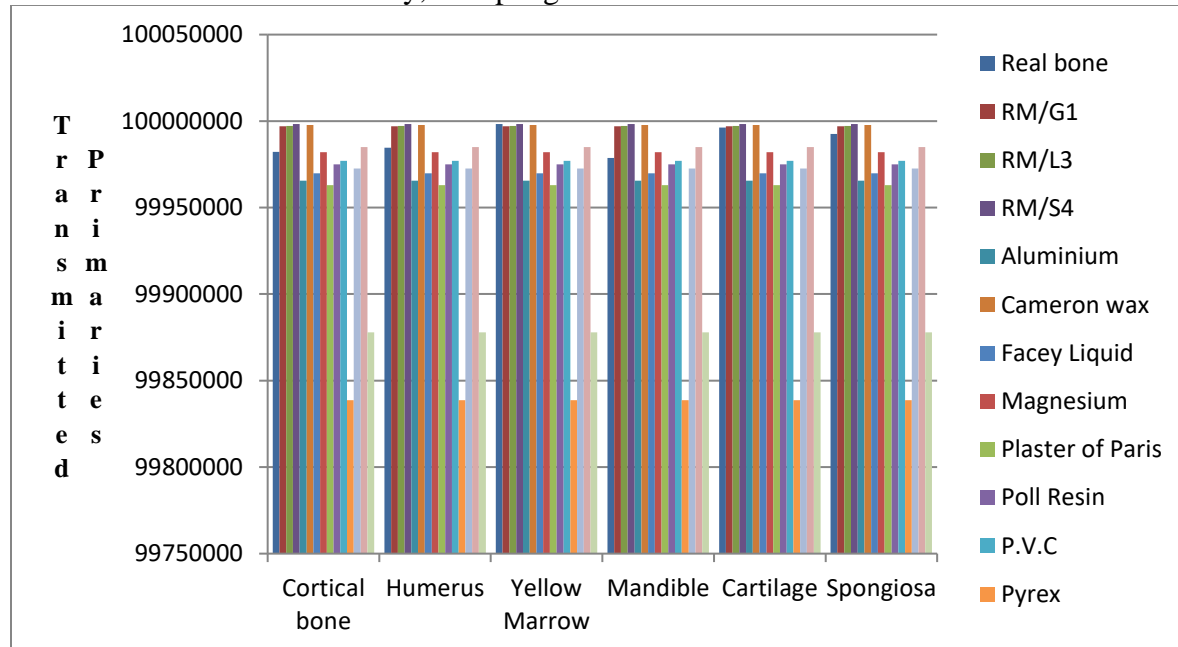


Fig. 2: The comparison of the number of photons transmitted as Primary scatter for the real bone tissues and bone tissue equivalent materials

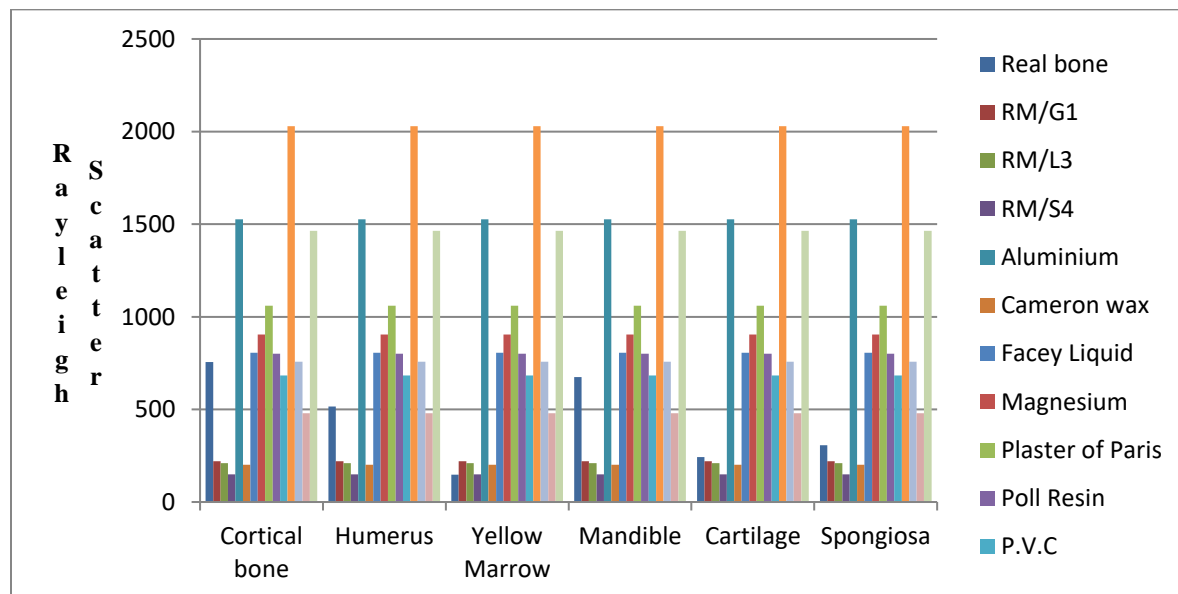


Fig. 3: The comparison of the number of photons transmitted as Rayleigh scatter for the real bone tissues and bone tissue equivalent materials



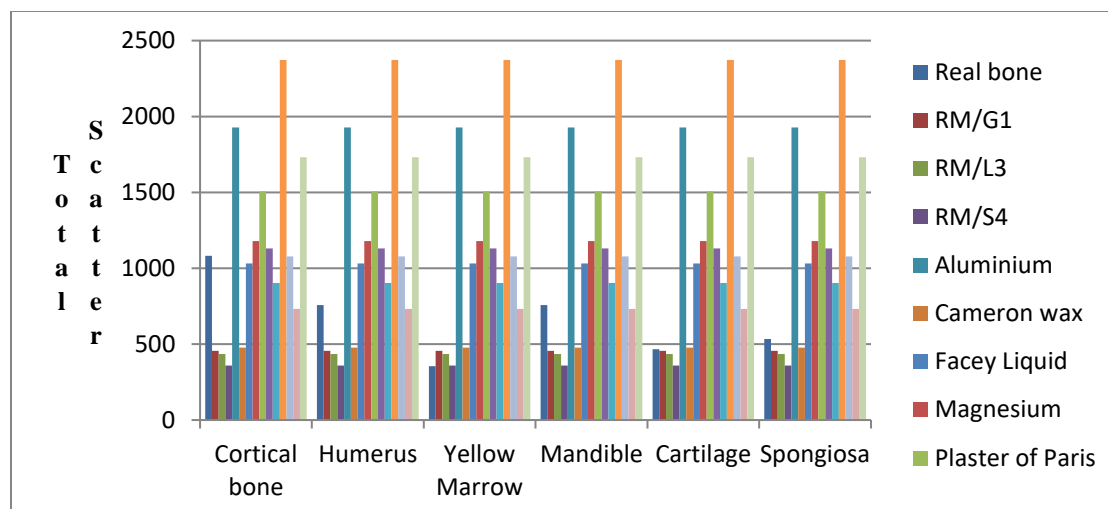


Fig. 4: The comparison of the number of photons transmitted as Total scatter for the real bone tissues and bone tissue equivalent materials

Figs. 2 to 4 show that magnesium and Poll resin exhibit the least percentage difference when compared to the real bone tissue (cortical bone) among the studied bone tissue substitutes (magnesium, Poll resin, Spiers Liquid, and Cameron wax). This suggests that magnesium and Poll resin have a closer resemblance to cortical bone. Furthermore, their scattering properties align well with cortical bone, as their peak positions occur at the same momentum transfer value (x) in Fig. 1, and they do not show significant discrepancies at low momentum transfer values.

Similarly, Figs. 2 to 4 indicate that magnesium and Poll resin also exhibit the least percentage difference when compared to the humerus (real bone tissue), whereas Spiers Liquid and Cameron wax deviate significantly. However, despite their relatively lower percentage difference, the overall results suggest that all the studied substitutes, including magnesium, Poll resin, Spiers Liquid, and Cameron wax, are poor simulators of humerus tissue. This is due to inconsistencies in the parameters used for characterization, leading to varying percentage differences across Figs. 2, 3, and 4. In this preliminary investigation, Shonka plastic was identified as the only suitable substitute for mandible bone tissue, whereas pyrex, Poll resin, and Spiers Liquid were found

to be poor simulators due to their large percentage differences from real bone tissue. Additionally, RM/G1, RM/L3, and Cameron wax exhibited the least percentage difference when compared to cartilage, suggesting that they can effectively simulate it. Conversely, P.V.C and Shonka Plastic are poor substitutes for cartilage due to their significant percentage difference.

Figs. 2 to 4 further show that RM/S4 and Cameron wax have the least percentage difference when compared to yellow marrow, with their peak positions occurring at the same momentum transfer value (x) in Fig. 1. This suggests that RM/S4 and Cameron wax can adequately simulate the scattering properties of yellow marrow.

However, all the bone tissue substitutes studied showed a significant percentage difference when compared to spongiosa (real bone). This indicates that none of the tested materials serve as effective simulators for spongiosa.

4.0 Conclusion

The X-ray diffraction patterns obtained in this study were in good agreement relative to previous measurements in terms of peak position. The computational results reported above shows that the scattering properties of some of the bone tissue equivalent materials are similar to some of the real bone tissues. It



revealed that magnesium and poll resin bone tissue substitutes can be used to simulate the cortical bone tissue while Spiers liquid and Cameron wax are not adequate to simulate the tissue. It was revealed that RM/G1, RM/L3 and Cameron wax bone tissue substitutes can be used to simulate the Cartilage bone tissue while PVC and shonka plastic are bad simulators. From the results too, RM/S4 and Cameron wax bone tissue substitutes can be used as good substitute for Yellow marrow bone tissue while Pyrex is a bad simulator. It was possible to identify Shonka plastic (B100) as the only good substitute for the Mandible bone tissue while Pyrex, poll resin and spiars liquid are bad simulators because of the wide percentage difference between it and the bone tissue substitutes studied. Based on wide disparity in the scattering properties/profiles obtained in this work, it was not possible to identify a good substitute for humerus, mandible and spongiosa.

5.0 References

- Barroso, R. C., Lopes, R. T., Goncalves, O. D., & de Assis, J. T. (2000). Angle-dispersive diffraction with synchrotron radiation at Laboratorio Nacional de Luz Sincrotron (Brazil): Potential for use in biomedical imaging. *Applied Radiation and Isotopes*, 53, pp. 717–724.
- Bozkurt, A., Çakal, G. Ö., Kaya-Keleş, Ş., & Kaşkaş, A. (2023). Comparison of h-BN material with metal implants in radiotherapy applications: Characterization and dose distribution measurements in LINAC. *Radiation Physics and Chemistry*, 212, pp. 111152. <https://doi.org/10.1016/j.radphyschem.2023.111152>.
- Chaparian, A., Oghabian, M. A., & Changizi, V. (2009). Acquiring molecular interference functions of X-ray coherent scattering for breast tissues by combination of simulation and experimental methods. *Iranian Journal of Radiation Research*, 7, 2, pp. 113–117.
- Evans, S. H., Bradley, D. A., Dance, D. R., Bateman, J. E., & Jones, C. H. (1991). Measurement of small-angle photon scattering for some breast tissues and tissue substitute materials. *Physics in Medicine & Biology*, 36, 1, pp. 7–18.
- Ferreira, C. C., Ximenes Filho, R. E. M., Vieira, J. W., Tomal, A., Poletti, M. E., Garcia, C. A. B., & Maia, A. F. (2010). Evaluation of tissue-equivalent materials to be used as human brain tissue substitutes in dosimetry for diagnostic radiology. *Physics in Medicine & Biology*, 55, pp. 2515–2521.
- Fewell, T. R., Shuping, R. E., & Hawkins, K. R. Jr. (1981). *Handbook of computed tomography X-ray spectra* (HHS Publication No. FDA 81-8162).
- Harding, G., Kosanetzky, J., Knoerr, B., & Neitzel, U. (1987). X-ray diffraction measurement of some plastic materials and body tissues. *Medical Physics*, 14, 4, pp. 1811–1816.
- Huamani, Y. T., Mullisaca, A. P., Apaza, G. V., Chen, F., & Vega, J. R. (2019). Construction and characterization of materials equivalent to the tissues and organs of the human body for radiotherapy. *Radiation Physics and Chemistry*, 159, pp. 70–75. <https://doi.org/10.1016/j.radphyschem.2019.01.013>
- International Commission on Radiation Units and Measurements (ICRU). (1989). *Tissue substitutes in radiation dosimetry and measurement* (ICRU Report No. 44). Bethesda, MD.
- International Commission on Radiation Units and Measurements (ICRU). (1992). *Photon, electron, proton, and neutron interaction data for body tissues* (ICRU Report No. 46). Bethesda, MD.
- Kawrakow, I., & Rogers, D. W. O. (2000). *The EGSnrc code system: Monte Carlo simulation of electron and photon transport* (Technical Report No. PIRS-



701). National Research Council of Canada.

Kawrakow, I., & Rogers, D. W. O. (2003). *The EGSnrc code system: Monte Carlo simulation of electron and photon transport* (pp. 1–289). National Research Council of Canada.

Kidane, G., Speller, R. D., Royle, G. J., & Hanby, A. M. (1999). X-ray scatter signatures for normal and neoplastic breast tissues. *Physics in Medicine & Biology*, 44, pp. 1791–1802.

Poletti, M. E., Goncalves, O. D., & Mazzaro, I. (2004). Measurements of X-ray scatter signatures for some tissue-equivalent materials. *Nuclear Instruments and Methods in Physics Research B*, 213, pp. 595–598.

Sibilano, T. L., De Caro, D., Altamura, D., Siliqi, D., Ramella, M., Boccafoschi, F., Ciasca, G., Campi, G., Tirinato, L., Di Fabrizio, E., & Giannini, C. (2014). An optimized table-top small-angle X-ray scattering set-up for nanoscale structural analysis of soft matter.

Swanson, T. (1953). *National Bureau of Standards (US), Circular 539*.

Compliance with Ethical Standards

Declaration

Ethical Approval

Not Applicable

Competing interests

The authors declare no known competing financial interests

Data Availability

Data shall be made available on request

Conflict of Interest

The authors declare no conflict of interest

Ethical Considerations

This study adhered to ethical guidelines for biomedical research and did not involve human or animal subjects requiring institutional approval. All materials used as bone tissue substitutes were commercially available or synthesized following standard laboratory protocols, ensuring compliance with safety and ethical standards. The research was conducted with transparency, and no conflicts of interest or ethical breaches were encountered in data collection, analysis, or reporting..

Funding

The authors declared no external source of funding

Authors' Contributions

KKO, CNO designed the work. CFJ, COI, UAE, MMO and CLK were involved in field work, data analysis and drafting of the manuscript

Authors' Contributions

KKO and ODO: Conceptualization, methodology, graphical plots and data analysis. NIA and KKO: Writing original draft, editing, proofreading and manuscript handling. KKO: Supervision and initial corrections. All the authors read and approved the final manuscript.

